RESEARCH ARTICLE | APRIL 16 2018

Epitaxial engineering of polar ε-Ga_2O_3 for tunable two-dimensional electron gas at the heterointerface FREE

Sung Beom Cho ; Rohan Mishra

Appl. Phys. Lett. 112, 162101 (2018)
https://doi.org/10.1063/1.5019721
CHORUS

Epitaxial engineering of polar ε-Ga_2O_3 for tunable two-dimensional electron gas at the heterointerface

Sung Beom Cho[1,a] and Rohan Mishra[1,2,a]
[1]*Department of Mechanical Engineering and Materials Science, Washington University in St. Louis, St. Louis, Missouri 63130, USA*
[2]*Institute of Materials Science and Engineering, Washington University in St. Louis, St. Louis, Missouri 63130, USA*

(Received 15 December 2017; accepted 1 April 2018; published online 16 April 2018)

We predict the formation of a polarization-induced two-dimensional electron gas (2DEG) at the interface of ε-Ga_2O_3 and $CaCO_3$, wherein the density of the 2DEG can be tuned by reversing the spontaneous polarization in ε-Ga_2O_3, for example, with an applied electric field. ε-Ga_2O_3 is a polar and metastable ultra-wide band-gap semiconductor. We use density-functional theory (DFT) calculations and coincidence-site lattice model to predict the region of epitaxial strain under which ε-Ga_2O_3 can be stabilized over its other competing polymorphs and suggest promising substrates. Using group-theoretical methods and DFT calculations, we show that ε-Ga_2O_3 is a ferroelectric material where the spontaneous polarization can be reversed through a non-polar phase by using an electric field. Based on the calculated band alignment of ε-Ga_2O_3 with various substrates, we show the formation of a 2DEG with a high sheet charge density of $10^{14}\,cm^{-2}$ at the interface with $CaCO_3$ due to the spontaneous and piezoelectric polarization in ε-Ga_2O_3, which makes the system attractive for high-power and high-frequency applications. *Published by AIP Publishing.*
https://doi.org/10.1063/1.5019721

Ga_2O_3 is emerging as an attractive semiconductor for high-power switching applications due to its high breakdown field and ultra-wide bandgap.[1–4] Amongst the various polymorphs of Ga_2O_3, the β-phase has received the most attention due to its stable form under ambient conditions and the ease of growing large single crystals.[5–7] Recently, carrier confinement and formation of a two-dimensional electron gas (2DEG) have been experimentally demonstrated at the interface of Ga_2O_3 with a wider bandgap alloy $(Al_xGa_{1-x})_2O_3$ by using modulation doping with silicon,[8] which enables Ga_2O_3-based devices to simultaneously operate at high-power and high-frequencies.[9–11] However, modulation doping results in a modest 2DEG density of $\sim 10^{12}\,cm^{-2}$ compared to a 2DEG density of $\sim 10^{13}\,cm^{-2}$ at the AlGaN/GaN interface.[12] Furthermore, it lowers the mobility of the 2DEG due to impurity scattering. These have led to a search for alternative ways to generate 2DEG in Ga_2O_3.[13]

Recently, ferroelectric hysteresis has been reported in thin films of ε-Ga_2O_3, which is a metastable polymorph.[14] Contrary to 2DEG formation in β-Ga_2O_3, the spontaneous polarization of ε-Ga_2O_3 can open a path to achieve 2DEG with high mobility and, possibly, higher sheet charge density without doping. While there have been numerous attempts to grow ε-Ga_2O_3 on various substrates,[15–17] they have been unsuccessful to grow single-phase thin films that are free of defects.[18] This is primarily due to a lack of understanding of the stability of the competing phases of Ga_2O_3 under epitaxial strain. Very recently, ε-Ga_2O_3 thin films have been stabilized on (001) Al_2O_3 substrates by using tin dopants during growth;[19] however, the formation of a 2DEG was not reported. This is because the formation of a 2DEG at the interface of ε-Ga_2O_3 with its lattice-matched substrate, such that the 2DEG resides in the semiconducting ε-Ga_2O_3, also requires a specific band alignment and the knowledge of its spontaneous and piezoelectric polarization constants, all of which are currently missing.

In this letter, we have investigated the energy landscape of various Ga_2O_3 polymorphs under epitaxial strain by combining coincident-site lattice models (CSL) with first-principles density-functional theory (DFT) calculations. We have identified the lattice parameter of the substrates that minimize the epitaxial strain of ε-Ga_2O_3 with respect to other competing phases and recommend a list of commercially available substrates to grow phase-pure ε-Ga_2O_3 without doping. By using group-theoretical methods, we show that ε-Ga_2O_3 is ferroelectric and the polarity of ε-Ga_2O_3 can be switched with an external electric field. Furthermore, by calculating the band alignment of the various lattice-matched substrates, we identify $CaCO_3$ to be particularly promising as it allows the formation of a 2DEG in ε-Ga_2O_3 due to polarization-induced charges. Finally, we show that an electric field can be used to switch the spontaneous polarization in ε-Ga_2O_3 to obtain a large charge density of $10^{14}\,cm^{-2}$. Therefore, by stabilizing an ultrawide bandgap semiconducting ferroelectric and an electric-field tunable 2DEG, our work paves a way to achieve a new generation of devices.

DFT calculations were performed using the VASP package[20] and projector augmented-wave potentials.[21] The plane-wave basis set was expanded to a cutoff energy of 520 eV to minimize Pulay stress during the structural optimization. The structural optimization was truncated after the Hellmann-Feynman forces were under 0.001 eV/Å. The Brillouin zone was sampled using the Monkhorst-Pack method with *k*-points grids of $6 \times 6 \times 2$ for α-, $13 \times 4 \times 4$ for β-, and $6 \times 4 \times 4$ for

[a]Authors to whom correspondence should be addressed: cho.s@wustl.edu and rmishra@wustl.edu

the transformed cell of the ε-phase under epitaxial strain, respectively.[23] The 3*d*, 4*s*, and 4*p* states of Ga and 2*s* and 2*p* states of O are taken as valence states, and the exchange-correlation energy of valence electrons was described using the Perdew, Burke, and Ernzerhof (PBE) functional.[22] As PBE is known to overestimate the lattice constants, to maintain consistency, we have used PBE-optimized lattice constants for all the substrate candidates, which are shown in supplementary material Table S3.[24] To calculate polarization constants, we used the Berry-phase method with a *k*-point grid of 6×4 with 16-point strings.[25] To evaluate the dielectric, piezoelectric, and stiffness constants, we employed density functional perturbation theory with an increased cutoff energy of 700 eV.[26] The bandgaps and electron affinities were calculated using the Heyd-Scuseria-Ernzerhof (HSE) hybrid functionals with a mixing parameter of 0.35 and 0.15 to fit the experimental bandgaps of β-Ga_2O_3 (Eg = 4.9 eV) and $CaCO_3$ (Eg = 6.0 eV), respectively.[27–30] Due to the lack of experimental measurements of the bandgap of high-quality ε-Ga_2O_3, combined with the similar theoretical bandgap of ε-Ga_2O_3 and β-Ga_2O_3 calculated using PBE (0.06 eV difference), we have used $\alpha = 0.35$ to calculate the bandgap of ε-Ga_2O_3. The *k*-point grid of substrate candidates was sampled with a density of 2000 *k*-points per reciprocal atom. The electron affinities were calculated using the electrostatic potential of non-polar $CaCO_3$ (104) and ε-Ga_2O_3 (010) surfaces with the macroscopic electrostatic potential averaging technique. To simulate the surfaces, we used slabs that were thicker than 25 Å and were separated by 20 Å vacuum.[31,32]

ε-Ga_2O_3 belongs to the $Pna2_1$ space group that is a subgroup of hexagonal $P6_3mc$. It implies that the orthorhombic lattice can be expressed with a basis transformation from the hexagonal lattice. The calculated $a = 5.13$ Å and $b = 8.81$ Å lattice parameters of ε-Ga_2O_3 have a ratio of $1.718 \approx \sqrt{3}$ that also corresponds to the ratio of the two diagonals of the rhombohedral lattice. According to CSL theory,[33] the epitaxial interface should be constrained such that a repeating unit is formed where the lattice sites of the film and the substrate coincide. Therefore, the (001) plane is promising as it can satisfy the CSL conditions for epitaxial growth on a hexagonal substrate (supplementary material Fig. S1). On the other hand, β-Ga_2O_3 does not have a coincidence lattice with a hexagonal substrate for small epitaxial strains. The reported preferred orientation of β-Ga_2O_3 on hexagonal substrates is the $(\bar{2}01)$ plane, which has calculated in-plane lattice vectors of 3.09 Å for the [010] direction and 14.98 Å for the $[10\bar{1}]$ direction and needs at least 7% strain to fit hexagonal constraints. Furthermore, the large difference of the two in-plane vectors in β-Ga_2O_3 requires a large CSL leading to a number of dangling bonds. ε-Ga_2O_3 can, instead, form a CSL with a smaller unit cell on a hexagonal substrate. This is beneficial to stabilize metastable ε-Ga_2O_3 over stable β-Ga_2O_3. We have also considered the CSL of α-Ga_2O_3, which is less stable compared to the ε and β phases in the bulk form[5] but has a hexagonal structure and could be expected to be stabilized on hexagonal substrates. The crystal structure of the α, β, and ε-phases of Ga_2O_3 is shown in Fig. 1(a).

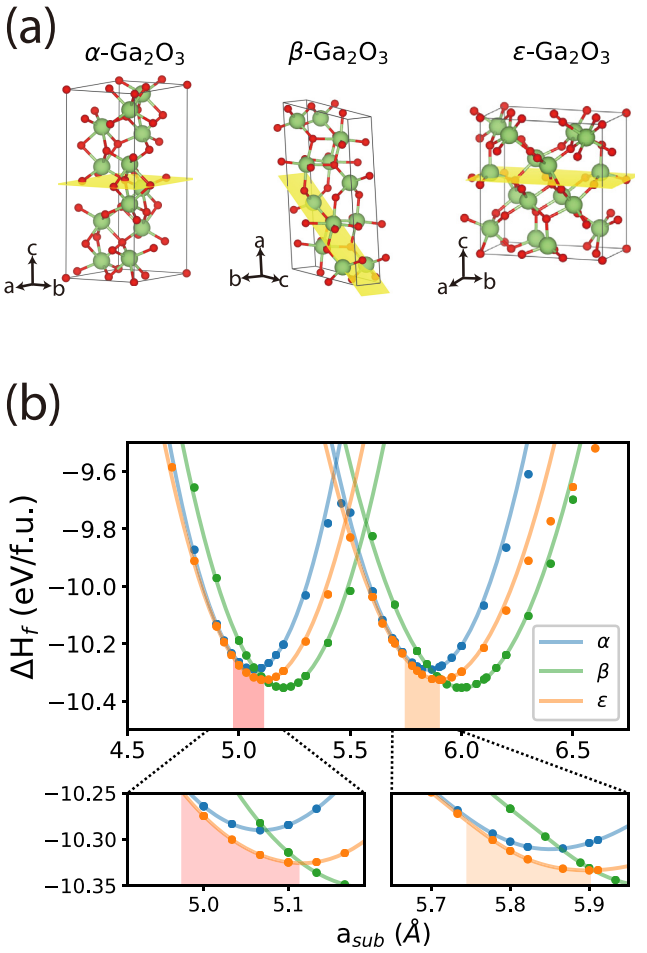

FIG. 1. (a) Atomic structure of α, β, and ε-Ga_2O_3 along the preferred lattice orientation on a hexagonal substrate. Green and red atoms represent Ga and O, respectively. The yellow plane represents the growth plane. (b) Strain energetics on a hexagonal (001) substrate and cubic (111) substrate. The shaded boxes highlight the regions where the epitaxial strain on ε-Ga_2O_3 along the [100] direction is under 3% and ε-Ga_2O_3 is more stable than the two other polymorphs.

We have calculated the energy of the preferred orientation of α, β, and ε-phases of Ga_2O_3 on hexagonal substrates as a function of varying lattice constants of the substrate, as shown in Fig. 1(b). For epitaxial stabilization of ε-Ga_2O_3, on hexagonal substrates, it should have the lowest energy amongst the three competing phases. Furthermore, the lattice mismatch with the substrate should be small, usually within ±3% in the case of oxides,[34] to avoid formation of defects caused by strain relaxation. With these constraints, we find hexagonal substrates matching the smallest CSL with ε-Ga_2O_3 and having a lattice constant between 4.97 and 5.12 Å to be most promising. Based on the calculated phase diagram under epitaxial strain, we find that previously used substrates to grow epitaxial ε-Ga_2O_3 impose strains over 3% or stabilize the α or β phases, which explains the poor quality of the deposited thin films (see supplementary material).[18] Based on the identified region of stability of ε-Ga_2O_3, we searched the Materials Project database[35] and suggest promising substrates in Table I. We find that non-polar substrates, such as α-Fe_2O_3, $CaCO_3$, *h*-BN, and SiO_2, are also commercially available. As discussed below, we find that $CaCO_3$ is particularly promising to induce 2DEG

TABLE I. Calculated commercially available substrates whose lattice mismatch with ε-Ga_2O_3 is under $\pm 3\%$. The lattice constants and the resulting strain have been calculated using the PBE functional.

Substrate	Lattice constant (Å)	Strain
α-Fe_2O_3	5.066	−1.19%
$LiTaO_3$	5.19	1.23%
$CaCO_3$	5.06	−1.31%
$LiNbO_3$	5.212	1.65%
h-BN	2.512	−2.01%
α-SiO_2	5.024	−2.04%

in ε-Ga_2O_3 due its large bandgap of 6.0 eV and favorable band alignment.[27]

We now focus on identifying the polar properties of ε-Ga_2O_3 and examine whether it is indeed possible to obtain ferroelectric switching to explain the hysteretic behavior reported in recent experiments.[14] Bulk ε-Ga_2O_3 belongs to the non-centrosymmetric $Pna2_1$ space group. Using Berry-phase calculations, we find that ε-Ga_2O_3 has a spontaneous polarization (P_{SP}) of 23 μC/cm^2 oriented along the *c*-axis, which is in good agreement with a recent theoretical report.[13] The calculated P_{SP} of ε-Ga_2O_3 is ten times larger than that of pyroelectric wide bandgap semiconductor GaN (2.9 μC/cm^2).[36] To switch the dipole moment in ε-Ga_2O_3 to the opposite direction, a transition through an intermediate centrosymmetric (non-polar) supergroup of the $Pna2_1$ space group is required. Using group-theoretical techniques, as implemented in the Pseudo and Amplimodes programs in the Bilbao crystallographic server,[37–39] we have identified *Pnna*, *Pccn*, *Pbcn*, and *Pnma* as the four centrosymmetric supergroups from which $Pna2_1$ can be obtained with minimal atomic distortion. Amongst them, we find that the transition from *Pbcn* to $Pna2_1$ space group involves the smallest displacement of all atoms along the Γ_3^- polar phonon mode and has the smallest energy barrier (E_b) of 0.95 eV, as shown in Fig. 2 (see supplementary material Fig. S2 for other transition pathways). This is a relatively large activation barrier comparable to that

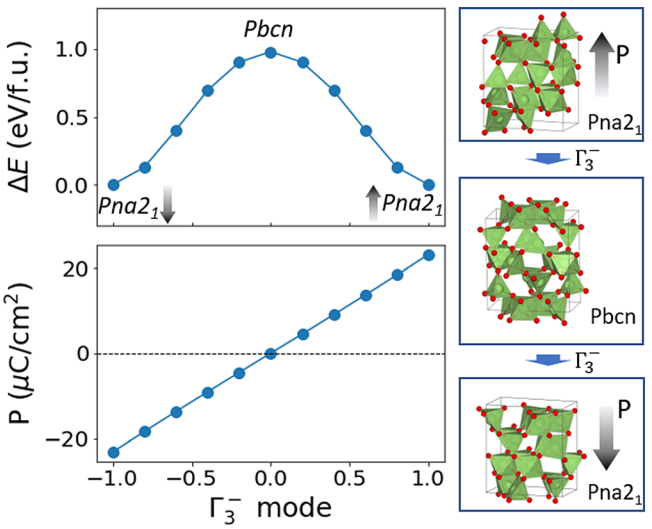

FIG. 2. The activation energy and spontaneous polarization along the transition path of ε-Ga_2O_3. The figures on the right show the atomic structure of the polar states with the opposite direction of the dipole moment and the intermediate non-polar phase.

of $GaFeO_3$ (1.05 eV), which shows a high ferroelectric to paraelectric transition temperature of 1368 K.[40] Such a high activation barrier is expected to stabilize the polarization against thermally activated random dipole switching even at high temperatures during operation, which makes ε-Ga_2O_3 an attractive ferroelectric semiconductor with an ultrawide bandgap.

In addition to P_{SP}, the use of an epitaxial strain to stabilize ε-Ga_2O_3 is expected to induce piezoelectric polarization (P_{PE}). For a non-polar substrate, the termination of polarization at the substrate/ε-Ga_2O_3 interface will induce a charge density (σ) with contributions from both P_{SP} and P_{PE} that can be expressed by[41]

$$\sigma = P_{SP} + P_{PE} = P_{SP} + e_{31}\epsilon_1 + e_{32}\epsilon_2 + e_{33}\epsilon_3, \quad (1)$$

where e_{31}, e_{32} and e_{33} are the piezoelectric constants, ϵ_1 and ϵ_2 are the two in-plane strains, and ϵ_3 is the out-of-plane strain on ε-Ga_2O_3 due to the substrate. The out-of-plane strain can be obtained using the elastic constants of ε-Ga_2O_3: $\epsilon_3 = -\epsilon_1 c_{13}/c_{33} - \epsilon_2 c_{23}/c_{33}$. The calculated piezoelectric and elastic constants are shown in Table II. We find that the piezoelectric constants are comparable to III–V semiconductors. For instance, e_{33} and e_{31} in GaN are 0.73 and −0.49, respectively.[36] Due to the magnitude of e_{31} and e_{33}, even small epitaxial strains can produce a large P_{PE}.

We use $CaCO_3$ as the substrate and calculate the charge density at the interface with ε-Ga_2O_3. $CaCO_3$ imposes a compressive strain of 1.4%, which leads to $P_{PE} = -49$ μC/cm^2, which has an opposite sign to that of P_{SP} (23 μC/cm^2) and points towards the substrate. While P_{PE} is fixed by the choice of the substrate, P_{SP} is switchable by an external electric field. Thereby, depending on the orientation of P_{SP} in ε-Ga_2O_3, the total polarization can be varied from −26 μC/cm^2 ($P_{PE} + P_{SP}$) to −72 μC/cm^2 ($P_{PE} - P_{SP}$). The corresponding sheet charge density (σ) varies between 1.6×10^{14} cm^{-2} and 4.4×10^{14} cm^{-2}, respectively, which is higher than the density present at AlGaN/GaN[41] and modulation-doped β-Ga_2O_3/Si:$(Al_xGa_{1-x})_2O_3$ heterojunctions.[9–11] Furthermore, the ferroelectric nature of ε-Ga_2O_3 is expected to allow the modulation of the charge density with an external electric field.

To identify the conditions under which the above calculated interface charges are expected to be mobile as opposed to being fixed, we have analyzed the band alignment and potential shift for different P_{SP} and thicknesses of ε-Ga_2O_3 films on the $CaCO_3$ substrate. The polarization in ε-Ga_2O_3 is associated with an internal electric field and potential-shift along the [001] direction. Based on the calculated dipole moment in a unit cell of ε-Ga_2O_3, the potential-shift can be estimated as[42–44]

$$\Delta V = -4\pi e \frac{(P_{SP} + P_{PE})c}{\varepsilon}. \quad (2)$$

TABLE II. Calculated piezoelectric constants and elastic constants of bulk ε-Ga_2O_3.

e_{31} (μC/cm^2)	e_{32} (μC/cm^2)	e_{33} (μC/cm^2)	c_{31} (GPa)	c_{32} (GPa)	c_{33} (GPa)
9.5	7.9	−16.3	125	125	207

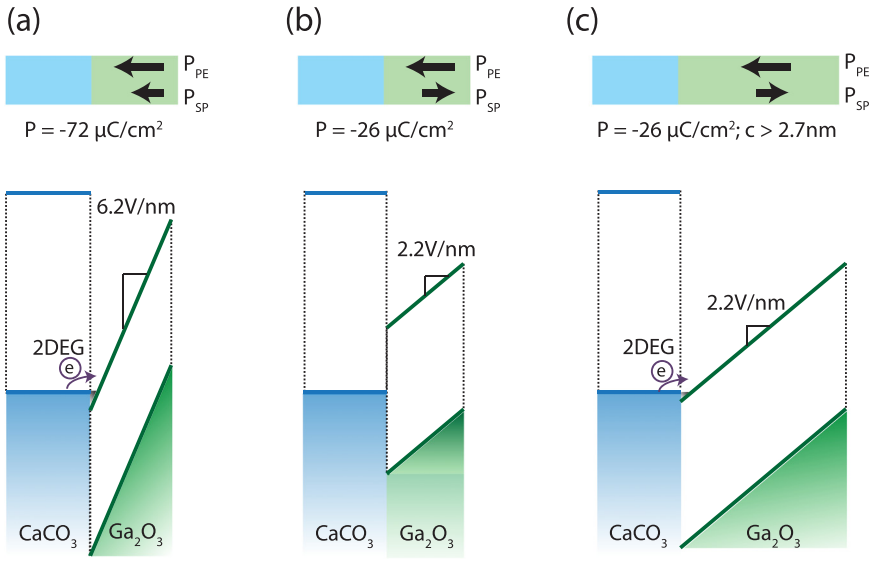

FIG. 3. Band alignment at the ε-Ga_2O_3(001)/$CaCO_3$(104) interface. Below the critical thickness of ε-Ga_2O_3, which is 2.7 nm (a) mobile 2DEG is expected to form with $P_{PE} - P_{SP}$ but not for (b) $P_{PE} + P_{SP}$. (c) Above the critical thickness, mobile 2DEG will form even for $P_{PE} + P_{SP}$.

Here, c is the lattice vector along the [001] direction (9.424 Å) of ε-Ga_2O_3 and ε is its calculated static dielectric constant (13.2). The potential shift ΔV of pristine ε-Ga_2O_3 without any strain ($P_{PE} = 0$) is -1.98 V/nm. The potential shift ΔV of strained ε-Ga_2O_3 on the $CaCO_3$ substrate is 2.23 V/nm for $P_{PE} + P_{SP}$ and 6.17 V/nm $P_{PE} - P_{SP}$. Therefore, it depends on the direction of P_{SP}, which can be controlled with an external electric field. With an optimal band alignment between the two materials, the large potential shift can be exploited such that the electrons from the valence band of $CaCO_3$ spontaneously ionize and spillover to the conduction band of ε-Ga_2O_3 to form a mobile 2DEG at the interface, as shown in Fig. 3. We have calculated band alignment between ε-Ga_2O_3 and the $CaCO_3$ substrate based on their bulk bandgap, electron affinity, and potential shift. We find that the two materials form a staggered gap of 2.86 eV at the heterointerface (supplementary material), where the band alignment is determined by the Anderson rule without considering the polarity.[45] Figure 3 shows the schematic band alignment at the ε-Ga_2O_3(001)/$CaCO_3$(104) interface and the different spontaneous polarization and thicknesses of ε-Ga_2O_3 under which a mobile 2DEG is expected to form. The direction of the total polarization is always towards the substrate as it is determined by P_{PE}, regardless of the direction of P_{SP}. For a thin layer of ε-Ga_2O_3 (<2.7 nm), if P_{SP} is parallel to P_{PE} (i.e., $P_{PE} + P_{SP}$), the strong field of 6.17 V/nm drives the conduction band of ε-Ga_2O_3 above the valence band of $CaCO_3$. This results in ionization of the valence electrons of $CaCO_3$ and a mobile 2DEG on the ε-Ga_2O_3 side. On the other hand, when the P_{SP} is switched such that it is antiparallel to P_{PE} (i.e., $P_{PE} - P_{SP}$), the interface charges are confined to the valence band of ε-Ga_2O_3 and are expected to be immobile. For ε-Ga_2O_3 films with the thickness above 2.7 nm, mobile 2DEG is expected for both the directions of P_{SP}; however, the sheet charge density can be tuned between 1.6×10^{14} cm^{-2} and 4.4×10^{14} cm^{-2} with an external electric field. We would like to point out that the exact sheet charge density and the critical thickness for the formation of 2DEG will also depend on the quality of the heterointerface, including the presence of defects and intermixing as is observed in the 2DEG formed at the $LaAlO_3$/$SrTiO_3$ heterointerface.[46–48]

In conclusion, we have investigated a pathway to stabilize metastable, polar ε-Ga_2O_3 using epitaxial strain and have identified promising substrate candidates. We have also calculated possible switching pathways for ε-Ga_2O_3 and predict it to be a ferroelectric wide bandgap semiconductor. Furthermore, we predict the formation of 2DEG at the interface of ε-Ga_2O_3 with $CaCO_3$ substrates with a sheet charge density that is two orders of magnitude higher than that obtained using modulation doping in β-Ga_2O_3/$(Al_xGa_{1-x})_2O_3$. Due to the ferroelectric nature of ε-Ga_2O_3, we show that the interface 2DEG density can be modulated using an external electric field, which opens a pathway to design new device architectures. The polarization-induced 2DEG in ε-Ga_2O_3 is also expected to result in devices that can simultaneously operate at high-power and high frequencies.

See supplementary material for the choice of CSL, the effect of PBE functional, and further substrate candidates for the epitaxial growth.

We are thankful to Prof. Sriram Krishnamoorthy of University of Utah for helpful discussions. This work used computational resources of the Extreme Science and Engineering Discovery Environment (XSEDE), which was supported by National Science Foundation Grant No. ACI-1053575.

[1]M. A. Mastro, A. Kuramata, J. Calkins, J. Kim, F. Ren, and S. J. Pearton, ECS J. Solid State Sci. Technol. **6**(5), P356–P359 (2017).
[2]M. Higashiwaki, K. Sasaki, H. Murakami, Y. Kumagai, A. Koukitu, A. Kuramata, T. Masui, and S. Yamakoshi, Semicond. Sci. Technol. **31**(3), 034001 (2016).
[3]M. Higashiwaki, K. Sasaki, A. Kuramata, T. Masui, and S. Yamakoshi, Appl. Phys. Lett. **100**(1), 013504 (2012).
[4]A. J. Green, K. D. Chabak, E. R. Heller, R. C. Fitch, M. Baldini, A. Fiedler, K. Irmscher, G. Wagner, Z. Galazka, S. E. Tetlak, A. Crespo, K. Leedy, and G. H. Jessen, IEEE Electron Device Lett. **37**(7), 902–905 (2016).
[5]S. Yoshioka, H. Hayashi, A. Kuwabara, F. Oba, K. Matsunaga, and I. Tanaka, J. Phys.: Condens. Matter **19**(34), 346211 (2007).
[6]A. Hideo, N. Kengo, T. Hidetoshi, A. Natsuko, S. Kazuhiko, and Y. Yoichi, Jpn. J. Appl. Phys., Part 1 **47**(11R), 8506 (2008).
[7]R. Roy, V. G. Hill, and E. F. Osborn, J. Am. Chem. Soc. **74**(3), 719–722 (1952).
[8]S. Krishnamoorthy, Z. Xia, S. Bajaj, M. Brenner, and S. Rajan, Appl. Phys. Express **10**(5), 051102 (2017).

[9]T. Oshima, Y. Kato, N. Kawano, A. Kuramata, S. Yamakoshi, S. Fujita, T. Oishi, and M. Kasu, Appl. Phys. Express **10**(3), 035701 (2017).
[10]S. Krishnamoorthy, Z. Xia, C. Joishi, Y. Zhang, J. McGlone, J. Johnson, M. Brenner, A. R. Arehart, J. Hwang, S. Lodha, and S. Rajan, Appl. Phys. Lett. **111**(2), 023502 (2017).
[11]E. Ahmadi, O. S. Koksaldi, X. Zheng, T. Mates, Y. Oshima, U. K. Mishra, and J. S. Speck, Appl. Phys. Express **10**(7), 071101 (2017).
[12]K. S. Im, J. B. Ha, K. W. Kim, J. S. Lee, D. S. Kim, S. H. Hahm, and J. H. Lee, IEEE Electron Device Lett. **31**(3), 192–194 (2010).
[13]M. B. Maccioni and V. Fiorentini, Appl. Phys. Express **9**(4), 041102 (2016).
[14]F. Mezzadri, G. Calestani, F. Boschi, D. Delmonte, M. Bosi, and R. Fornari, Inorg. Chem. **55**(22), 12079–12084 (2016).
[15]H. Nishinaka, D. Tahara, and M. Yoshimoto, Jpn. J. Appl. Phys. **55**(12), 1202BC (2016).
[16]Y. Oshima, E. G. Víllora, Y. Matsushita, S. Yamamoto, and K. Shimamura, J. Appl. Phys. **118**(8), 085301 (2015).
[17]X. Xia, Y. Chen, Q. Feng, H. Liang, P. Tao, M. Xu, and G. Du, Appl. Phys. Lett. **108**(20), 202103 (2016).
[18]I. Cora, F. Mezzadri, F. Boschi, M. Bosi, M. Čaplovičová, G. Calestani, I. Dódony, B. Pécz, and R. Fornari, CrystEngComm **19**(11), 1509–1516 (2017).
[19]M. Kracht, A. Karg, J. Schörmann, M. Weinhold, D. Zink, F. Michel, M. Rohnke, M. Schowalter, B. Gerken, A. Rosenauer, P. J. Klar, J. Janek, and M. Eickhoff, Phys. Rev. Appl. **8**(5), 054002 (2017).
[20]G. Kresse and J. Furthmüller, Phys. Rev. B **54**(16), 11169 (1996).
[21]P. E. Blöchl, Phys. Rev. B **50**(24), 17953 (1994).
[22]J. P. Perdew, K. Burke, and M. Ernzerhof, Phys. Rev. Lett. **77**(18), 3865–3868 (1996).
[23]H. J. Monkhorst and J. D. Pack, Phys. Rev. B **13**(12), 5188 (1976).
[24]P. Haas, F. Tran, and P. Blaha, Phys. Rev. B **79**(8), 085104 (2009).
[25]R. King-Smith and D. Vanderbilt, Phys. Rev. B **47**(3), 1651 (1993).
[26]M. Gajdoš, K. Hummer, G. Kresse, J. Furthmüller, and F. Bechstedt, Phys. Rev. B **73**(4), 045112 (2006).
[27]D. R. Baer and D. L. Blanchard, Appl. Surf. Sci. **72**(4), 295–300 (1993).
[28]Y. Kang, K. Krishnaswamy, H. Peelaers, and C. G. Van de Walle, J. Phys. Condens. Matter **29**(23), 234001 (2017).
[29]A. V. Krukau, O. A. Vydrov, A. F. Izmaylov, and G. E. Scuseria, J. Chem. Phys. **125**(22), 224106 (2006).
[30]J. Heyd, G. E. Scuseria, and M. Ernzerhof, J. Chem. Phys. **118**(18), 8207–8215 (2003).
[31]V. Stevanovic, S. Lany, D. S. Ginley, W. Tumas, and A. Zunger, Phys. Chem. Chem. Phys. **16**(8), 3706–3714 (2014).
[32]Y. Hinuma, Y. Kumagai, F. Oba, and I. Tanaka, Comput. Mater. Sci. **113**, 221–230 (2016).
[33]W. Bollmann, *Crystal Defects and Crystalline Interfaces* (Springer, 1970).
[34]D. G. Schlom, L.-Q. Chen, C. J. Fennie, V. Gopalan, D. A. Muller, X. Pan, R. Ramesh, and R. Uecker, MRS Bull. **39**(2), 118–130 (2014).
[35]A. Jain, S. P. Ong, G. Hautier, W. Chen, W. D. Richards, S. Dacek, S. Cholia, D. Gunter, D. Skinner, G. Ceder, and K. A. Persson, APL Mater. **1**(1), 011002 (2013).
[36]F. Bernardini, V. Fiorentini, and D. Vanderbilt, Phys. Rev. B **56**(16), R10024–R10027 (1997).
[37]D. Orobengoa, C. Capillas, M. I. Aroyo, and J. M. Perez-Mato, J. Appl. Crystallogr. **42**, 820–833 (2009).
[38]J. M. Perez-Mato, D. Orobengoa, and M. I. Aroyo, Acta Crystallogr. A **66**, 558–590 (2010).
[39]C. Capillas, E. S. Tasci, G. de la Flor, D. Orobengoa, J. M. Perez-Mato, and M. I. Aroyo, Z. Kristallogr.-Cryst. Mater. **226**(2), 186–196 (2011).
[40]S. Song, H. M. Jang, N.-S. Lee, J. Y. Son, R. Gupta, A. Garg, J. Ratanapreechachai, and J. F. Scott, NPG Asia Mater. **8**, e242 (2016).
[41]R. Mishra, O. D. Restrepo, S. Rajan, and W. Windl, Appl. Phys. Lett. **98**(23), 232114 (2011).
[42]R. Pentcheva and W. E. Pickett, Phys. Rev. Lett. **102**(10), 107602 (2009).
[43]J. Lee and A. A. Demkov, Phys. Rev. B **78**(19), 193104 (2008).
[44]W.-J. Son, E. Cho, B. Lee, J. Lee, and S. Han, Phys. Rev. B **79**(24), 245411 (2009).
[45]R. Anderson, IBM J. Res. Dev. **4**(3), 283–287 (1960).
[46]H. Chen, A. M. Kolpak, and S. Ismail-Beigi, Adv. Mater. **22**(26–27), 2881–2899 (2010).
[47]C. Cantoni, J. Gazquez, F. Miletto Granozio, M. P. Oxley, M. Varela, A. R. Lupini, S. J. Pennycook, C. Aruta, U. S. di Uccio, P. Perna, and D. Maccariello, Adv. Mater. **24**(29), 3952–3957 (2012).
[48]J. Gazquez, M. Stengel, R. Mishra, M. Scigaj, M. Varela, M. A. Roldan, J. Fontcuberta, F. Sánchez, and G. Herranz, Phys. Rev. Lett. **119**(10), 106102 (2017).